Cloaking and enhanced scattering of core-shell plasmonic nanowires

Ali Mirzaei,* Ilya V. Shadrivov, Andrey E. Miroshnichenko, and Yuri S. Kivshar

Nonlinear Physics Center and Center for Ultra-high bandwidth Devices for Optical Systems (CUDOS), Research School of Physics and Engineering, Australian National University, Canberra ACT 0200, Australia

*amz124@physics.anu.edu.au

Abstract: We study scattering of light from multi-layer plasmonic nanowires and reveal that such structures can demonstrate both enhanced and suppressed scattering regimes. We employ the mode-expansion method and experimental data for material parameters and introduce an optimized core-shell nanowire design which exhibits simultaneously superscattering and cloaking properties at different wavelengths in the visible spectrum.

OCIS codes: (250.5403) Plasmonics; (240.3695) Linear and nonlinear light scattering from surfaces; (230.3205) Invisibility cloaks.

References and links

1. N. I. Zheludev and Y. S. Kivshar, "From metamaterials to metadevices," Nat. Mater. **11**, 917–924 (2012).
2. A. Alu and N. Engheta, "Achieving transparency with plasmonic and metamaterial coatings," Phys. Rev. E **72**, 016623 (2005).
3. A. Alu and N. Engheta, "Multifrequency optical invisibility cloak with layered plasmonic shells," Phys. Rev. Lett. **100**, 113901 (2008).
4. A. A. Zharov and N. A. Zharova, "On the electromagnetic cloaking of (nano)particles," Bull. Russ. Acad. Sci.: Physics **74**, 89–92 (2010).
5. D. S. Filonov, A. P. Slobozhanyuk, P. A. Belov, and Y. S. Kivshar, "Double-shell metamaterial coatings form plasmonic cloaking," Phys. Status Solidi RRL **6**, 46–48 (2012).
6. P. Y. Chen, J. Soric, and A. Alu, "Invisibility and cloaking based on scattering cancellation," Adv. Mater. **24**, OP281–304 (2012).
7. Z. Ruan and S. Fan, "Temporal coupled-mode theory for fano resonance in light scattering by a single obstacle," J. Phys. Chem. C, **114**, 7324–7329 (2010).
8. Z. Ruan and S. Fan, "Superscattering of light from subwavelength nanostructures," Phys. Rev. Lett. **105**, 013901 (2010).
9. Z. Ruan and S. Fan, "Design of subwavelength superscattering nanospheres," Appl. Phys. Lett. **98**, 043101 (2011).
10. L. Verslegers, Z. Yu, Z. Ruan, P. B. Catrysse, and S. Fan, "From electromagnetically induced transparency to superscattering with a single structure: a coupled-mode theory for doubly resonant structures," Phys. Rev. Lett. **108**, 083902 (2012).
11. P. Fan, U. K. Chettiar, L. Cao, F. Afshinmanesh, N. Engheta, and M. L. Brongersma, "An invisible metalsemiconductor photodetector," Nat. Photonics **6**, 380–385 (2012)
12. D. Rainwater, A. Kerkhoff, K. Melin, J. C. Soric, G. Moreno, and A. Al, "Experimental verification of three-dimensional plasmonic cloaking in free-space," New J. Phys. **14**, 013054 (2012)
13. B. Edwards, A. Al, M. G. Silveirinha, and N. Engheta, "Experimental verification of plasmonic cloaking at microwave frequencies with metamaterials," Phys. Rev. Lett. **103**, 153901 (2009)
14. C. A. Balanis, *Advanced engineering electromagnetics* (Wiley, 1989).
15. M. I. Tribelsky and B. S. Luk'yanchuk, "Anomalous light scattering by small particles," Phys. Rev. Lett. **97**, 263902 (2006).
16. E. Palik, *Handbook of optical constants of solids* (Academic Press, 1997).

#185835 - $15.00 USD Received 22 Feb 2013; revised 26 Mar 2013; accepted 2 Apr 2013; published 22 Apr 2013

17. U. Kreibig, "Electronic properties of small silver particles: the optical constants and their temperature dependence," J. Phys. F: Metal Phys. **4**, 999–1014 (1974).
18. S. A. Maier, *Plasmonics: fundamentals and applications* (Springer, 2007).

1. Introduction

Recent growing interest in study of optical metamaterials is explained by their unusual properties such as negative refraction, perfect lensing, zero refractive index, and invisibility cloaking which can be employed for many useful functionalities of *metadevices* [1]. These studies stipulated some parallel activities in nanoplasmonics, where similar properties were found for metal-dielectric subwavelength structures. In particular, it was shown that multi-shell plasmonic nanoparticles may possess highly unusual scattering characteristics related to the reduced scattering which can be associated with invisibility cloaking [2–5] based on scattering cancellation [6, 7]. In addition to cloaking, it was shown that multi-layer nanoparticles can exhibit the enhanced scattering (called *superscattering* [8–10]) when the SCS of a subwavelength structure exceeds substantially its geometrical cross-section and even can be made arbitrary large.

These two seemingly different phenomena have been shown for different nanoparticles with quite dissimilar shell structure, and very often under the assumption of low losses. We wonder if the predicted effects of the anomalous scattering, i.e. the enhanced and suppressed scattering (superscattering and cloaking) *may exist for realistic parameters* and if these two dissimilar effects can be observed in one type of structure.

Cloaking of metal-dielectric cylindrical structures has been investigated experimentally by combining geometrically resonant metallic and semiconductor nanostructures with highly functional hybrid devices that derive their properties from the near-field coupling via intermodal interference and local negative polarizability [11–13]. In this paper, we analytically study these interference effects by considering the role of realistic material dispersion and losses on both superscattering and cloaking of multi-shell nanowires. First, we analyse the scattering properties of a three-layer structure (Fig. 1(a)) and demonstrate that for realistic parameters the previously predicted superscattering regime is drastically suppressed. Then, using experimental data, we introduce a simple design of a nanoplasmonic structure (Fig. 1(b)) which demonstrates both superscattering and cloaking effects in the visible frequency spectrum.

2. Model and parameters

We study the scattering properties of two types of layered plasmonic nanowires shown schematically for their cross-sections in Fig. 1. Each of these structures has a metal core and one or two shells (the structure (a) has an extra coating metallic layer). We assume that the structures are placed in air and study the scattering of TM electromagnetic waves with the magnetic field polarized along the axis of cylinders. To describe the interaction of an incident plane wave as $\mathbf{H}^{Inc} = \hat{\mathbf{a}}_z H_0 e^{-i\omega t + i2\pi\lambda^{-1} r\cos(\varphi)}$ with the structure, we use the multipole expansion method. In a L-layered cylindrical structure, the total field in layer l can be presented as

$$\mathbf{H}^l_{total} = \hat{\mathbf{a}}_z H_0 e^{-i\omega t} \sum_{n=-\infty}^{+\infty} \exp\left(in\left[\varphi + \tfrac{\pi}{2}\right]\right)\left[\tau^l_n J_n\left(m^l(r)\right) + \rho^l_n H^{(1)}_n\left(m^l(r)\right)\right],$$

where $m^l(r) = 2\pi r\lambda^{-1}[\varepsilon_l(\lambda)]^{\frac{1}{2}}$, H_0 is the incident wave amplitude, J_n and $H^{(1)}_n$ are the n-th order Bessel and Hankel functions of the first kind, respectively; n is the mode number, $\varepsilon_l(\lambda)$ is the dielectric constant of the l-th layer at wavelength λ, r is the radius within the layer l, τ^l_n and ρ^l_n are n-th mode expansion coefficients in the l-th layer which are found by solving the boundary condition equations for the tangential components H_z and E_φ. Additionally, we put

#185835 - $15.00 USD Received 22 Feb 2013; revised 26 Mar 2013; accepted 2 Apr 2013; published 22 Apr 2013

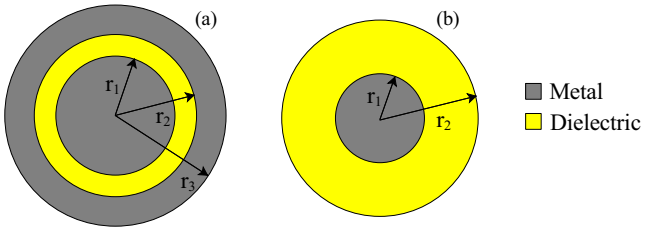

Fig. 1. Schematic view of (a) double-shell and (b) core-shell nanowires.

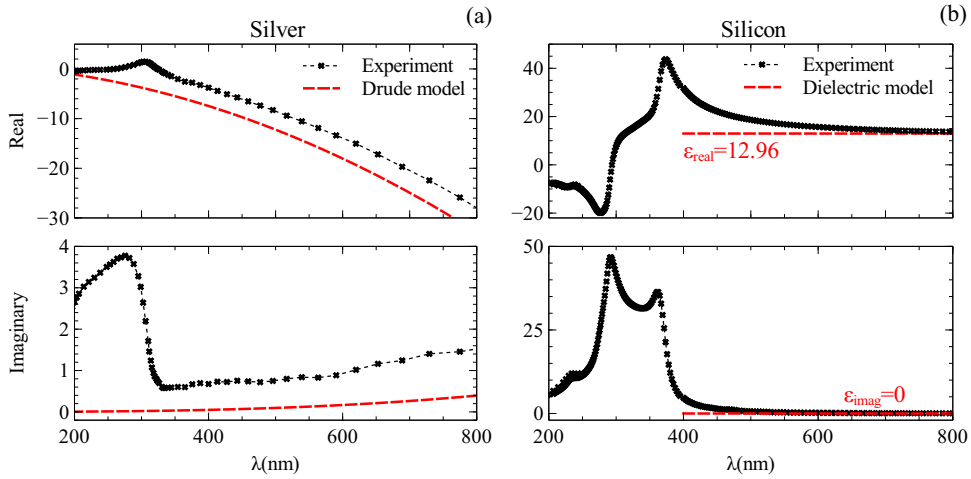

Fig. 2. Real and imaginary parts of dielectric permittivity of bulk (a) silver and (b) silicon. (a) Comparison of the permittivity for silver with experimental data and modelled with the Drude formula. (b) Silicon experimental data vs. commonly used a constant value of 12.96.

$\rho_n^1 = 0$ to avoid singularity of Hankel functions at the origin, and $\tau_n^{L+1} = 1$ for each mode, to describe the incident plane wave expansion through the cylindrical waves.

The total scattering cross-section (SCS) is defined as a ratio of the total scattered power to the intensity of the incident plane wave, and in our case it can be found as [14]:

$$SCS = \frac{2\lambda}{\pi\sqrt{\varepsilon_{L+1}}} \sum_{n=-\infty}^{+\infty} |\rho_n^{L+1}|^2$$

where we observe that multiple modes can contribute to SCS. At the same time, if only a dipole mode is excited (the so-called single-channel scattering), then the SCS maximum in a nanowire (two-dimensional) geometry is $4\lambda/\pi$ (taking into account $|\rho_n^{L+1}| = |\rho_{-n}^{L+1}|$ degeneracy) [8, 15]. We follow [8] and normalize all SCS values to $2\lambda/\pi$ introducing *normalized scattering cross-section* (NSCS). Employing multi-layered structures with plasmonic materials, the value of SCS can be significantly enhanced by employing multiple scattering channels. To achieve this, we need to design a nanostructure with a significant contribution of different channels *at a same frequency* by overlapping the frequencies of at least two different resonances [8, 10].

Metals are known to be strongly dispersive in the optical frequency spectrum. Therefore, it is important to use accurate models for describing metal properties in order to obtain realistic results. Here, we compare the results obtained by using Drude's model for silver (this model was employed in [8]) with the results obtained by using the experimental data from [16]. In

#185835 - $15.00 USD Received 22 Feb 2013; revised 26 Mar 2013; accepted 2 Apr 2013; published 22 Apr 2013

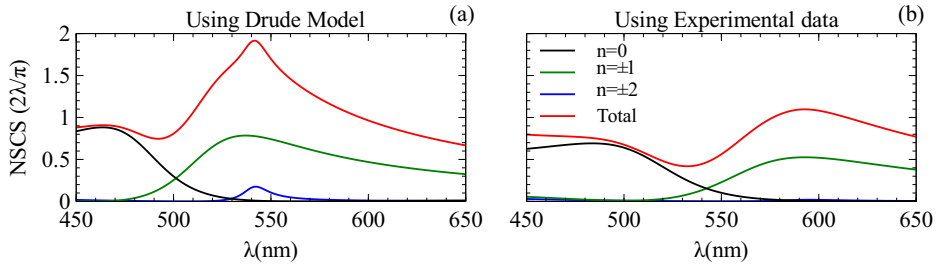

Fig. 3. NSCS of the 3-layer structure, using (a) Drude's model and (b) experimental data.

addition, for shorter wavelengths the permittivity of some common dielectrics also becomes dispersive and this effect will contribute to the light scattering.

Superscattering of a double-shell structure shown in Fig. 1(a) has been studied previously in [8], where $\varepsilon_d = 12.96$ is used as permittivity of the dielectric layer, as well as Drude's model for the permittivity of silver, $\varepsilon = \varepsilon_\infty - \omega_p^2/(\omega^2 + i\gamma\omega)$, where $\varepsilon_\infty = 1$, $\omega_p = 1.37 \cdot 10^{16}$ rad/sec and $\gamma = 2.74 \cdot 10^{13}$ rad/sec are plasma and bulk collision frequencies respectively (using additional surface damping as is followed). These dependences are shown by dashed lines in Fig. 2(a). The radii of the shells, $r_{1,2,3}$, are 47.9 nm, 77.3 nm, and 87.6 nm, respectively.

It is well known that small nanoparticles may have dielectric constants quite different from those of bulk materials [17]. In particular, when the size of a nanowire becomes comparable with the electron mean free path, the collision frequency is modified. To take into account this size-dependent effect, we modify the collision frequency of the Drude model γ [17], making the following replacement: $\gamma_{small-particle} = \gamma_{bulk} + AV_f/d$, where $A = 1$, $V_f = 1.388 \cdot 10^6$ m/s (the Fermi velocity in silver), and d is the characteristic size of the metallic structure. Taking this additional surface damping into account, the calculated NSCS as well as contributions to scattering from the first three modes, is shown in Fig. 3(a), and these results coincide with those of Fig. 4(a) in [8] (shown in a wider wavelength range).

However, Fig. 2(a) indicates that Drude's model does not describe accurately the experimental data for silver in the visible spectrum. For longer wavelengths these discrepancies can be reduced by using appropriate values of ε_∞, γ and ω_p. This, however, still does not describe the parameters of silver well enough for higher frequencies, namely above the interband transition frequency [18]. To demonstrate the importance of using accurate values of $\varepsilon_l(\lambda)$ in numerical simulations, below we study the light scattering by the same structure but using Palik's data for $\varepsilon_{silver}(\lambda)$ [16] and compare the results with those obtained using Drude's approximation.

To obtain the corrected dielectric permittivity of metals in nanoparticles using experimental data, we use real (ε_r) and imaginary (ε_i) parts of bulk material dielectric permittivity from [16] to achieve γ_{bulk} and ω_p by using the Drude formula as follows (here we use $\varepsilon_\infty^{silver} = 4.96$ [16]):

$$\gamma_{bulk} = \frac{\omega\varepsilon_i}{(\varepsilon_\infty - \varepsilon_r)} \quad , \quad \omega_p^2 = \omega^2 \frac{(\varepsilon_\infty - \varepsilon_r)^2 + \varepsilon_i^2}{\varepsilon_\infty - \varepsilon_r}.$$

Then by calculating $\gamma_{small-particle}$ we recover the value of ε using Drude's model (one also can use the approximation $\varepsilon_{small-particle} = \varepsilon_{bulk} + i[\omega_p^2 V_f]/[\omega^3 d]$).

Figure. 3 shows the NSCS results for a three-layer nanowire with the Drude model and Palik's experimental data for the metallic layer. The superscattering effect observed for Drude's model [Fig. 3(a)] completely disappears when we use experimental data, as shown in Fig. 3(b). This demonstrates the importance of using material realistic parameters. Moreover, at lower wavelengths, permittivity of dielectrics may also become significantly dispersive, as shown in Fig. 2(b) for silicon. In what follows, we use realistic dispersive data for both silver and

#185835 - $15.00 USD Received 22 Feb 2013; revised 26 Mar 2013; accepted 2 Apr 2013; published 22 Apr 2013

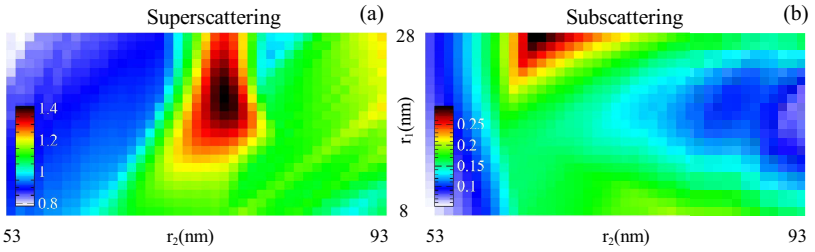

Fig. 4. (a) Maximum and (b) minimum values of NSCS of core-shell nanowire versus radii r_1 and r_2 in the visible wavelength region (380nm-750nm) using experimental data.

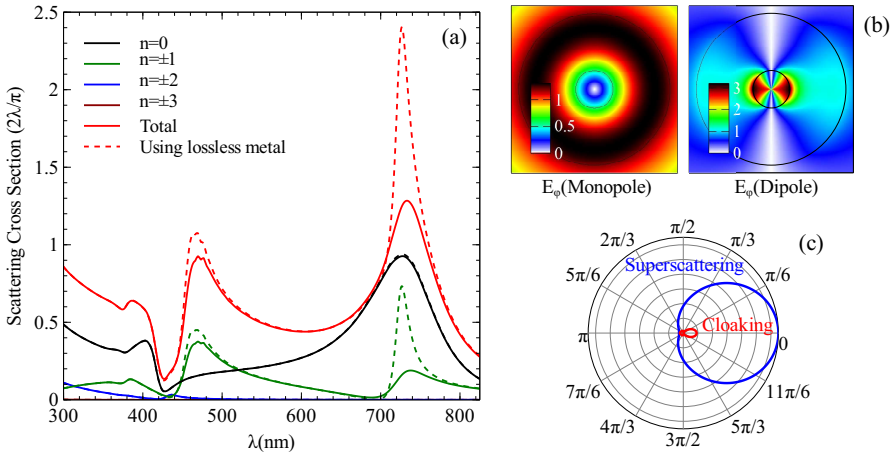

Fig. 5. (a) NSCS of a core-shell structure with cloaking and superscattering properties at 427 nm and 733 nm, respectively. Dotted lines show the results for the case of lossless metal. (b) Field profile (dipole and monopole modes) as the absolute values of E_φ normalized to the incident wave amplitude in superscattering regime using realistic parameters and (c) far-field radiation pattern of the nanowire with plane-wave excitation from left.

silicon, with a linear interpolation between experimental points where needed.

3. Superscattering and cloaking

These results obtained above rise an important question: *Is it still possible to observe enhanced scattering with layered nanowires for realistic materials?* Or, what is the realistic variation of the SCS of layered nanowires? To answer these questions we analyse the scattering properties of a simpler core-shell metal-dielectric structure shown in Fig. 1(b), which has silver core and silicon outer shell. In Fig. 4 we plot maximum and minimum NSCS within the frequency range of interest as a function of radii r_1 and r_2. We observe that the maximum NSCS close to 1.4 can be achieved in this structure. Moreover, if we take the values $r_1 = 18$ nm and $r_2 = 73$ nm, then both enhanced and suppressed scattering can be observed simultaneously. In particular, for such a choice of parameters, the NSCS is 0.135 at 426.9 nm and 1.284 at 733.2 nm. Corresponding NSCS is shown in Fig. 5(a) as a function of wavelength. The suppressed scattering is associated with the cloaking phenomenon, where the scattering of all modes is simultaneously and significantly reduced [2, 3]. At the same time, at the frequency of enhanced scattering, both monopole and dipole modes are at resonance. Remarkably, if we calculate NSCS neglecting metal losses

#185835 - $15.00 USD Received 22 Feb 2013; revised 26 Mar 2013; accepted 2 Apr 2013; published 22 Apr 2013

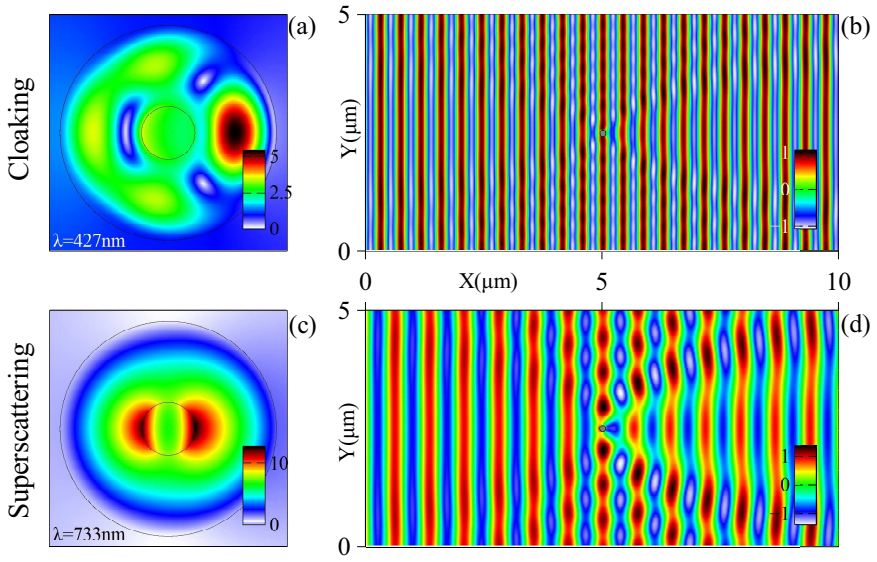

Fig. 6. Distribution of the magnetic field in cloaking (a,b) and superscattering (c,d) regimes for the plane wave incident from the left. The internal field profiles in (a,c) are shown as the absolute values of the total field H_z normalized to the incident wave amplitude. (b,d) Real part of H_z. The small grey circle in the plots (b,d) corresponds to the nanowire.

[shown by dashed curves in Fig. 5(a)], we obtain that losses predominantly suppress the dipole mode without affecting much the monopole mode. This effect originates from stronger overlap of the dipole mode with metallic part of the nanowire as shown in Fig. 5(b). Also as the dipole mode has a higher quality factor than the monopole mode, the light resides longer in the dipole mode of the nanowire and material loss has a higher impact in this mode. We also compare the directionality of the scattering in both the regimes, as shown in Fig. 5(c). In both cases, scattering occurs predominantly in the forward direction with a significant difference in amplitude which is quite attractive for applications to optical antennas.

Figure. 6 shows the near-field and scattered-field distribution inside and outside the nanowire in both enhanced and suppressed scattering regimes. In enhanced scattering regime the near-field exhibits superposition of monopole and dipole modes inside the nanowire as was expected from scattering cross section in this regime from Fig. 5(a).

4. Conclusions

We have demonstrated that previously predicted superscattering enhancement of plasmonic nanowires vanishes for experimental parameters of the metallic layers. This indicates a high sensitivity of the proposed effect to the material parameters and losses that hinders its practical realization. By analysing a simpler core-shell metal-dielectric nanowire, we have found a range of parameters where enhanced and reduced scattering (associated with cloaking) phenomena, can be observed simultaneously in the same structure in the visible spectral range.

Acknowledgments

The authors thank S. Fan and Z. Ruan for useful discussions and acknowledge a support from the Australian Research Council through the Future Fellowship, Discovery and Centre of Excellence programs.

#185835 - $15.00 USD Received 22 Feb 2013; revised 26 Mar 2013; accepted 2 Apr 2013; published 22 Apr 2013